ELSEVIER

Journal of Organometallic Chemistry 635 (2001) 9–23

Journal of Organometallic Chemistry

www.elsevier.com/locate/jorganchem

Understanding the nature of the bonding in transition metal complexes: from Dewar's molecular orbital model to an energy partitioning analysis of the metal–ligand bond☆

Gernot Frenking *

Fachbereich Chemie, Philipps-Universität Marburg, Hans-Meerwein- Strasse, D-35039 Marburg, Germany

Received 24 June 2001; accepted 1 August 2001

Abstract

The results of an energy partitioning analysis of three classes of transition metal complexes are discussed. They are (i) neutral and charged isoelectronic hexacarbonyls $TM(CO)_6^q$ ($TM^q = Hf^{2-}$, Ta^-, W, Re^+, Os^{2+}, Ir^{3+}); (ii) Group-13 diyl complexes $(CO)_4Fe$–ER (E = B, Al, Ga, In, Tl; R = Cp, Ph), $Fe(ECH_3)_5$ and $Ni(ECH_3)_4$; (iii) complexes with cyclic π-donor ligands $Fe(Cp)_2$ and $Fe(\eta^5\text{-}N_5)_2$. The results show that Dewar's molecular orbital model can be recovered and that the orbital interactions can become quantitatively expressed by accurate quantum chemical calculations. However, the energy analysis goes beyond the MO model and gives a much deeper insight into the nature of the metal–ligand bonding. It addresses also the question of ionic versus covalent bonding as well as the relative importance of σ and π bonding contributions.

Keywords: DFT; Molecular orbital calculations; Synergic bonding; Carbonyls; Group 13-diyl

1. Introduction

The history of chemistry knows a small number of chemical models which were first suggested in order to rationalise a single puzzling phenomenon but then they became the paradigmatic ground for a whole new area in chemistry. Classical examples are Kekulé's bonding model for benzene [1] and its quantum chemical explanation given by Hückel [2] which is the theoretical foundation of aromaticity and aromatic compounds [3] and the Woodward–Hoffmann/Fukui orbital symmetry rules [4] which gave an understanding for the reaction mechanism of pericyclic and other organic reactions [5]. Another equally important bonding model, which is now ubiquitously used in transition metal (TM) chemistry, was suggested by Dewar, who introduced in 1951 the concept of metal–ligand orbital interactions in terms of ligand → metal σ-donation and metal → ligand π-backdonation [6]. Dewar suggested the molecular orbital model to describe the bonding of an olefin coordinated to Ag(I) or Cu(I). A peculiar aspect of the groundbreaking idea is that Dewar apparently was not very interested in the field of TM chemistry and probably was not aware of the huge impact of his suggestion to the field. It was the famous paper by Chatt and Duncanson [7] who used Dewar's model for a systematic description of metal–olefin complexes which led to the breakthrough of Dewar's MO model in TM chemistry. This is the reason that the bonding model of donation and backdonation between a metal and a ligand is now termed the CDC model after Dewar, Chatt and Duncanson.

The DCD model has become the standard model not only for metal–olefin bonds but also for all kinds of transition metal–ligand bonds (TM–L). Textbooks of inorganic and organometallic chemistry and chemical bonding theory usually show the relevant molecular orbitals of the ligand and the metal or metal fragment and then discuss the bonding in terms of ligand → metal donation and metal → ligand backdonation [8]. This is done in a qualitative and heuristic way. The results are frequently compared with experimental values such as bond lengths, bond strengths and vibrational frequen-

☆ Theoretical studies of organometallic compounds. Part 47. Part 46: A. Kovàcs, G. Frenking, Organometallics 20 (2001) 2510.

* Tel.: +49-6421-2825563; fax: +49-6421-2825561.

E-mail address: frenking@chemie.uni-marburg.de (G. Frenking).

0022-328X/01/$ - see front matter
PII: S0022-328X(01)01154-8

cies. Calculations at the EHT level particularly by Hoffmann supported the DCD model [9]. EHT calculations have been used to discuss the bonding situation in numerous TM compounds providing the basis for a qualitative bonding model based on approximate quantum chemical methods [10].

The last decade has seen an enormous progress in quantum chemical methods for calculating TM compounds and other heavy atom molecules with high accuracy. This became possible because gradient corrected DFT, effective core potentials and new methods for calculating relativistic effects have been introduced at standard levels of theory which were proven to give accurate geometries, energies and other important properties of molecules [11]. Progress has also been made in the development of methods for analysing the electronic structure of the calculated species. New techniques were suggested for partitioning the electronic charge and the bonding energy of molecules. The natural bond orbital (NBO) method by Weinhold [12] and the topological analysis of the electron density distribution by Bader [13] are powerful tools which provide detailed insight into the bonding situation in a molecule. The charge decomposition analysis (CDA) is particularly interesting in the context of the DCD bonding model [14]. It is a charge partitioning method which calculates the amount of electronic charge of the ligand → metal donation and the metal → ligand backdonation for each orbital. The analysis of the bonding situation of many TM complexes showed that the DCD model of metal–ligand bonds can be quantitatively expressed using the results of the CDA calculations [15].

A perhaps even more important question concerns the energies which are associated with the ligand → metal donation and the metal → ligand backdonation. Energy partitioning methods such as the extended transition state (ETS) method developed by Ziegler and Rauk [16] and the related energy decomposition analysis (EDA) which was earlier suggested by Morokuma [17] are available which give well defined energy terms for the donation and backdonation. Thus, accurate quantum chemical calculations at the DFT or ab initio level may be used to obtain energy values which give the strength of the ligand → metal donation and the metal → ligand backdonation. The energy analysis may even be used in such a way that it goes beyond the DCD model. The first and perhaps most detailed investigation was made 10 years ago by Davidson et al. who analysed the chemical bonding in $Cr(CO)_6$ [18]. We could show in recent investigations that the partitioning of the total energy of a transition metal complex into energies of the bonding fragments may lead to expressions which can be interpreted only in terms of donation and backdonation [19–22]. While the latter considers only the orbital interactions as components of the TM–L bonds the energy partitioning also gives information about the relative strength of the electrostatic and orbital interactions. We proposed that the latter term may be considered as a measure of the covalent bonding while the former term gives the strength of the ionic bonding. The progress which has been made in the understanding of the chemical bond in transition metal complexes has recently been reviewed [23].

In this paper we compare recent results of the EDA of three classes of transition metal complexes. The data which were obtained in these studies show that, although the original bonding model which was suggested by Dewar 50 years ago is beautifully recovered and quantitatively supported by modern quantum chemical methods, other terms than donation and backdonation need to be considered for a full understanding of the chemical bond. The analysis shows that the metal–ligand interactions can be divided into three physically meaningful components whose strength can be quantitatively estimated. They are the attractive electrostatic interaction (ionic bonding), the attractive orbital interactions (covalent bonding) and the repulsive interactions between occupied orbitals of the fragments which arise from the Pauli repulsion. The DCD model is then given by the relative strength of the orbital interactions between occupied ligand orbitals and empty metal orbitals (donation) and between occupied metal orbitals and empty ligand orbitals (backdonation). Although the absolute values of the latter terms may not be the largest ones they often (but not always!) determine the trend of the bond strength. The three classes of TM complexes are: (i) carbonyls for which the isoelectronic series $TM(CO)_6^q$ ($TM^q = Hf^{2-}$, Ta^-, W, Re^+, Os^{2+}, Ir^{3+}) was chosen; (ii) carbonyl complexes with Group-13 diyl ligands $(CO)_4Fe–ER$ (E = B, Al, Ga, In, Tl; R = Cp, Ph) and homoleptical Group-13 diyl complexes $Fe(ECH_3)_5$ and $Ni(ECH_3)_4$; (iii) complexes with cyclic π-donor ligands $Fe(Cp)_2$ and $Fe(\eta^5\text{-}N_5)_2$. We will compare the most important results of the EDA. Further results such as the geometries and bond energies and a more detailed discussion of the bonding analysis are given in the original publications [20–22].

2. Methods

The calculations have been performed at the gradient corrected DFT level using the exchange functional of Becke [24] and the correlation functional of Perdew [25] (BP86). Relativistic effects have been considered in case of the carbonyls and for the complexes with cyclic π-donor ligands $Fe(Cp)_2$ and $Fe(\eta^5\text{-}N_5)_2$ by the zero-order regular approximation (ZORA) [26]. The Group-13 diyl complexes $(CO)_4Fe–ER$ have been calculated using

the Pauli formalism [27]. Uncontracted Slater-type orbitals (STOs) were used as basis functions for the SCF calculations [28]. The basis sets for the metal atoms have triple-ζ quality, which are augmented by one set of 6p functions. Triple-ζ basis sets augmented by two sets of d-type polarisation functions have been used for carbon and oxygen. The core electrons of the main group elements up to $(n-1)s^2$ and $(n-1)p^6$, the $(1s2s2p)^{10}$ core electrons of Fe, Ni and the $(1s2s2p3s3p3d4s4p4d)^{46}$ core electrons of Hf–Ir were treated by the frozen-core approximation [29]. An auxiliary set of s, p, d, f and g STOs was used to fit the molecular densities and to represent the Coulomb and exchange potentials accurately in each SCF cycle [30]. The optimised structures have been verified as minima on the potential energy surface by calculation of the vibrational frequencies. All calculations were carried out with the program package ADF [31].

The bonding interactions either between the metal fragment L'_nTM and a single ligand L or between the bare metal TM and the ligands L_n have been analysed with the energy decomposition scheme ETS developed by Ziegler and Rauk [16]. The bond dissociation energy ΔE between two fragments A and B is partitioned into several contributions which can be identified as physically meaningful entities. First, ΔE is separated into two major components ΔE_{prep} and ΔE_{int}:

$$\Delta E = \Delta E_{prep} + \Delta E_{int} \quad (1)$$

ΔE_{prep} is the energy which is necessary to promote the fragments A and B from their equilibrium geometry and electronic ground state to the geometry and electronic state which they have in the compound AB. ΔE_{int} is the instantaneous interaction energy between the two fragments in the molecule. The latter quantity shall be the focus of the present work. The interaction energy ΔE_{int} can be divided into three main components:

$$\Delta E_{int} = \Delta E_{elstat} + \Delta E_{Pauli} + \Delta E_{orb} \quad (2)$$

ΔE_{elstat} gives the electrostatic interaction energy between the fragments which are calculated with a frozen electron density distribution in the geometry of the complex. ΔE_{Pauli} gives the repulsive interactions between the fragments which are caused by the fact that two electrons with the same spin cannot occupy the same region in space. The term comprises the four-electron destabilising interactions between occupied orbitals. ΔE_{Pauli} is calculated by enforcing the Kohn–Sham determinant of AB, which results from superimposing fragments A and B, to be orthonormal through antisymmetrisation and renormalisation. The stabilising orbital interaction term ΔE_{orb} is calculated in the final step of the ETS analysis when the Kohn–Sham orbitals relax to the their form. The latter term can be further partitioned into contributions by the orbitals which belong to different irreducible representations of the interacting system.

We want to comment on the physical interpretation of the three terms given in Eq. (2). The first two terms ΔE_{elstat} and ΔE_{Pauli} are often added to a single term $\Delta E°$ which is sometimes called 'steric energy term' [32]. $\Delta E°$ has nothing to do with the loosely defined steric interaction which is often used to explain the repulsive interactions of bulky substituents. Since ΔE_{elstat} is usually attractive and ΔE_{Pauli} repulsive, the two terms cancel each other and the focus of the discussion of the bonding interactions then rests on the orbital interaction term ΔE_{orb}. This leads to the deceptive description of the bonding only in terms of orbital interactions. Because the orbital interactions can be associated with the covalent contributions to the bond and the electrostatic term with the ionic bonding the important information about the ionic/covalent character of the bond which is given by the ratio $\Delta E_{elstat}/\Delta E_{orb}$ is lost if only the sum of ΔE_{elstat} and ΔE_{Pauli} is given.

We want to emphasise that the calculation of the electrostatic interactions by integration of the charge distribution of the fragments takes care of the anisotropy of the electronic charge distribution of the atoms. The ionic character of a bond is frequently associated with the atomic partial charges. This can be misleading because the atomic partial charges give the total net charge of an atom without considering the special distribution of the electrons. Atoms, which carry an overall positive partial charge, may have areas of negative (electronic) charge concentration which can lead to attractive interactions with atoms that have a (local) positive charge. Examples of this will be given below.

3. Metal–CO bonding in $TM(CO)_6^q$ ($TM^q = Hf^{2-}$, Ta^-, W, Re^+, Os^{2+}, Ir^{3+}) [20]

The choice of the fragments for the analysis of the TM–CO bonding in the isoelectronic hexacarbonyls which are experimentally known was done in two different ways. One way was by analysing the interactions of a single CO ligand with the remaining $TM(CO)_5^q$ fragment. The other choice was by taking the metal atom as one fragment and the $(CO)_6$ ligand cage as the other fragment. We begin with the bonding analysis of one CO with $TM(CO)_5^q$. Fig. 1 shows the DCD model of the orbital interactions between the valence orbitals of CO and the metal TM. The dominant orbital interactions according to the DCD model should arise from the donation of the CO σ HOMO which is mainly a lone-pair orbital at carbon into the empty d_{z^2} metal AO, and the backdonation from the filled d(π) AO of the metal into the π* MO of CO.

Table 1 gives the calculated contributions of the energy terms which are given by Eqs. (1) and (2). The first three lines give the bond dissociation energies ΔE,

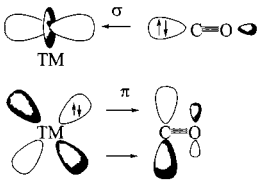

Fig. 1. Schematic representation of the TM–CO orbital interactions in carbonyl complexes. OC→TM σ-donation (top) and TM→CO π-backdonation (bottom).

the preparation energies ΔE_{prep} and the interaction energies ΔE_{int} according to Eq. (1). The calculated bond dissociation energies ΔE show an interesting U-shaped trend from $Hf(CO)_6^{2-}$ to $Ir(CO)_6^{3+}$ where the lowest ΔE value is predicted for neutral $W(CO)_6$. The values for ΔE_{prep} are small, because the frozen geometries of the fragments $TM(CO)_5^q$ and CO in the hexacarbonyls are not very different from the equilibrium structures [20]. The interaction energies ΔE_{int} of the frozen structures have the same U-shaped curve as the ΔE values. Thus, the partitioning of the energy terms given by Eq. (2) should give an explanation for the strange trend of ΔE_{int} and ΔE. One could speculate that the larger values of the highest charged species $Hf(CO)_6^{2-}$ and $Ir(CO)_6^{3+}$ might come from a higher degree of electrostatic interactions.

Lines 4–6 of the data in Table 1 give the three components of the ΔE_{int} term, i.e. the Pauli repulsion ΔE_{Pauli}, the electrostatic attraction ΔE_{elstat} and the orbital interactions ΔE_{orb}. There are three important points that we want to make. First, the repulsive Pauli term has always the largest absolute values of the three energy components. Second, the relative strength of the electrostatic (ionic) bonding contributions of the highly charged hexacarbonyls is *not* higher than in the less charged species. On the contrary, the energy analysis

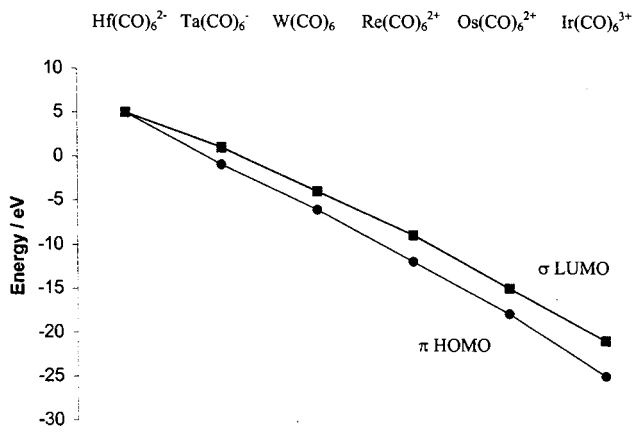

Fig. 2. Trend of the frontier orbital energy levels of the pentacarbonyls. Reproduced with permission from Ref. [20].

shows that the highest charged complexes $Hf(CO)_6^{2-}$ and $Ir(CO)_6^{3+}$ have the lowest degree of electrostatic bonding and thus, the highest degree of covalent bonding of the six molecules. The ETS analysis suggests that the $(CO)_5TM^q$–CO bonds have 55.4% covalent contributions when $TM^q = Hf^{2-}$ and 52.2% when $TM^q = Ir^{3+}$. An explanation for this paradoxical finding can be given when the change of the HOMO and LUMO eigenvalues of $TM(CO)_5^q$ are considered. They are shown in Fig. 2.

The trend of the calculated frontier orbital energies of $TM(CO)_5^q$ shows that the charge of the metal has a very strong influence on the HOMO and LUMO energies. There is a span of 25–30 eV between the frontier orbital energy values from the left to the right (Fig. 2). The doubly negatively charged $Hf(CO)_6^{2-}$ has a very high lying π HOMO which can strongly interact with the π* LUMO of CO. Table 1 shows that the π orbital interactions (orbitals with e symmetry) are very large in

Table 1
Energy decomposition and bonding analysis of $TM(CO)_5^q$+CO (kcal mol^{-1}) and calculated interatomic distances TM–C (Å) [a]

	$Hf(CO)_6^{2-}$	$Ta(CO)_6^{-}$	$W(CO)_6$	$Re(CO)_6^{+}$	$Os(CO)_6^{2+}$	$Ir(CO)_6^{3+}$
ΔE	−50.84	−48.26	−45.98	−48.36	−56.92	−73.74
ΔE_{prep}	5.75	3.05	3.65	4.38	5.00	5.16
ΔE_{int}	−56.59	−51.31	−49.63	−52.74	−61.92	−78.90
ΔE_{Pauli}	76.63	100.74	118.31	126.86	125.44	115.94
ΔE_{elstat} [b]	−59.38 (44.6%)	−76.56 (50.4%)	−90.08 (53.6%)	−97.69 (54.4%)	−98.48 (52.6%)	−93.08 (47.8%)
ΔE_{orb} [b]	−73.83 (55.4%)	−75.48 (49.6%)	−77.87 (46.4%)	−81.92 (45.6%)	−88.87 (47.4%)	−101.76 (52.2%)
A_1 [c]	−17.19 (23.3%)	−25.79 (34.3%)	−35.92 (46.1%)	−47.34 (57.8%)	−60.08 (67.6%)	−75.39 (74.2%)
A_2	0.00	0.00	0.00	0.00	0.00	0.00
B_1	0.05	0.02	−0.03	−0.07	−0.09	−0.10
B_2	−0.05	−0.07	−0.07	−0.07	−0.06	−0.05
E [c]	−56.64 (76.7%)	−49.64 (65.8%)	−41.85 (53.8%)	−34.44 (42.1%)	−28.64 (32.2%)	−26.22 (25.8%)
Distances						
TM–C	2.195	2.112	2.061	2.036	2.034	2.055

[a] Values taken from Ref. [20].
[b] Values in parentheses give the percentage of attractive interactions $\Delta E_{elstat}+\Delta E_{orb}$.
[c] Values in parentheses give the percentage of orbital interactions ΔE_{orb}.

Table 2
Energy decomposition analysis (kcal mol^{-1}) of $TM^q+(CO)_6$ [a]

	$Hf(CO)_6^{2-}$	$Ta(CO)_6^-$	$W(CO)_6$	$Re(CO)_6^+$	$Os(CO)_6^{2+}$	$Ir(CO)_6^{3+}$
ΔE_{int}	−543.90	−525.56	−473.89	−456.57	−544.40	−801.58
ΔE_{Pauli}	367.40	413.38	438.80	454.51	451.33	420.93
ΔE_{elstat} [b]	−358.62 (39.4%)	−397.62 (42.3%)	−396.24 (43.4%)	−375.09 (41.2%)	−353.44 (35.5%)	−337.81 (27.6%)
ΔE_{orb} [b]	−552.68 (60.6%)	−541.32 (57.7%)	−516.44 (56.6%)	−536.00 (58.8%)	−642.27 (64.5%)	−884.70 (72.4%)
A_{1g} [c]	−9.48 (1.7%)	−10.49 (1.8%)	−15.40 (2.8%)	−27.42 (4.6%)	−47.63 (6.4%)	−78.78 (7.5%)
A_{2g}	0.00	0.00	0.00	0.00	0.00	0.00
E_g [c]	−83.36 (14.6%)	−113.07 (20.3%)	−159.08 (29.3%)	−233.72 (39.6%)	−348.84 (46.9%)	−520.66 (49.5%)
T_{1g} [c]	−1.30 (0.3%)	−0.98 (0.2%)	−2.88 (0.5%)	−8.91 (1.5%)	−19.41 (2.6%)	−33.92 (3.2%)
T_{2g} [c]	−437.42 (76.6%)	−397.59 (71.2%)	−308.18 (56.8%)	−200.33 (34.0%)	−101.14 (13.6%)	−43.82 (4.2%)
A_{1u}	−0.03	−0.04	−0.03	0.00	−0.02	−0.02
E_u	0.00	−0.00	0.00	0.00	0.00	0.00
T_{2u} [c]	−2.74 (4.8%)	−2.00 (0.4%)	−4.35 (0.8%)	−11.60 (2.0%)	−23.86 (3.2%)	−40.17 (3.8%)
T_{1u} [c]	−18.35 (3.2%)	−17.15 (3.1%)	−26.52 (4.9%)	−54.00 (9.2%)	−101.37 (13.6%)	−167.33 (15.9%)
T_{1u} (σ)	−12.97	−12.06	−18.65	−38.53	−73.98	−125.68
T_{1u} (π)	−5.38	−5.09	−7.87	−15.47	−27.39	−41.65

[a] Taken from Ref. [20].
[b] Values in parentheses give the percentage of attractive interactions $\Delta E_{elstat}+\Delta E_{orb}$.
[c] Values in parentheses give the percentage of orbital interactions ΔE_{orb}.

the hafnium complex. The triply charged $Ir(CO)_6^{3+}$ has a very low lying σ LUMO (Fig. 2) which leads to very strong orbital interactions with the σ donor orbital of CO. Table 1 shows that the $(CO)_5TM^q \leftarrow CO$ σ donation (a_1 orbital interactions) are very strong in $Ir(CO)_6^{3+}$. The conclusion is that the charge of the complex has a much higher influence on the orbital interactions because of the change of the orbital energies than on the electrostatic interactions. The latter term shows a nice correlation with the calculated bond distances TM–CO which are given in the last line of Table 1.

The third point we want to emphasise is that none of the three energy components ΔE_{Pauli}, ΔE_{elstat} and ΔE_{orb} follows the trend of the ΔE_{int} and ΔE values exactly. Table 2 shows that the strength of the bonding interactions increase from neutral $W(CO)_6$ to the dianion $Hf(CO)_6^{2-}$ although neither of the attractive terms ΔE_{elstat} and ΔE_{orb} becomes larger when the hexacarbonyl becomes negatively charged. The stronger $(CO)_5TM^q$–CO bonds of the anions arise from the decrease of the repulsive term ΔE_{Pauli} (Table 2). The increase in ΔE_{int} from $W(CO)_6$ to $Ir(CO)_6^{3+}$, however, correlates nicely with the stronger orbital interaction term ΔE_{orb}. This is because the ΔE_{elstat} and ΔE_{Pauli} values of the cations make a nearly constant contribution to ΔE_{int}. The stronger electrostatic attraction of the cations is cancelled by the equally stronger Pauli repulsion. This is a coincidence which should not be used as evidence that the trend of the bond strengths depends only on the orbital interactions! The trend of the three energy components ΔE_{Pauli}, ΔE_{elstat} and ΔE_{orb} to the total interaction energy ΔE_{int} is graphically shown in Fig. 3.

The final set of ETS data which is given in Table 1 are the orbital interaction energies which arise from orbitals which have different symmetry. The ΔE_{orb} term has contributions from orbitals which have a_1, a_2, b_1, b_2 and e symmetry because $TM(CO)_5^q$ has C_{4v} symmetry. The a_1 contributions come from the $(CO)_5TM^q \leftarrow CO$ σ donation and the e contributions come from the $(CO)_5TM^q \rightarrow CO$ π backdonation [20]. Table 1 shows that the ΔE_{orb} values of the other orbitals are negligible. Previous investigations which analysed the bonding in neutral TM carbonyls showed that the π backdonation is in most cases stronger than the σ donation [34]. The ETS results of $W(CO)_6$ given in Table 1 agree with this. The π backdonation gives 53.8% of the orbital interaction energy while the σ donation gives only 46.2%. The latter contribution increases in the cations with up to 74.2% in $Ir(CO)_6^{3+}$ (25.8% backdonation) while the

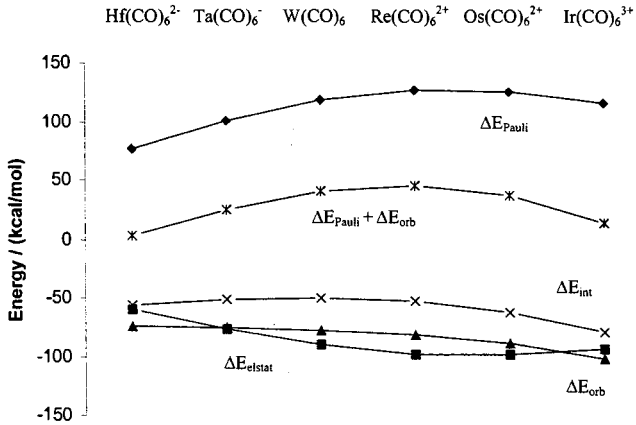

Fig. 3. Trend of the energy contributions to the interaction energy between $TMq(CO)_5$ and CO. Reproduced with permission from Ref. [20].

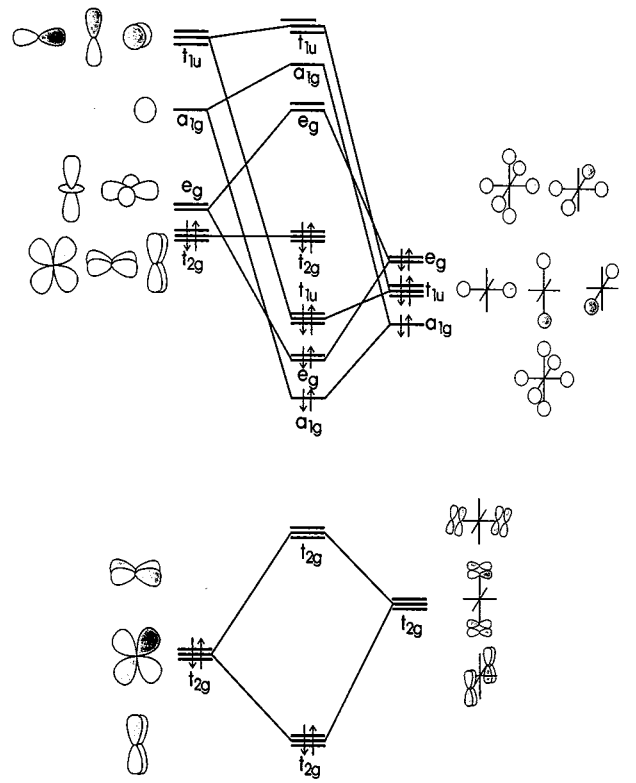

Fig. 4. Orbital interaction diagram of the splitting of the d, s, p valence orbitals of a transition metal in an octahedral ligand field. (a) Interactions of the σ orbitals; (b) interactions of the π orbitals.

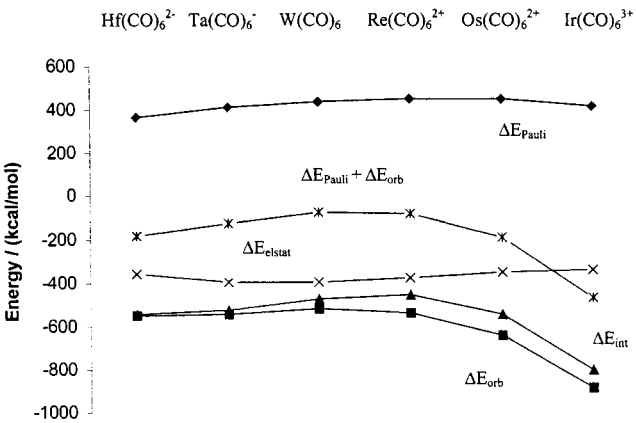

Fig. 5. Trend of the energy contributions to the interaction energy between TMq and $(CO)_6$. Reproduced with permission from Ref. [20].

backdonation clearly dominates the ΔE_{orb} interactions in the negatively charged complexes. The trend is easily understood when the orbital energies are considered (Fig. 2).

We also investigated the interactions between the bare metal atom TM^q and the ligand cage $(CO)_6$. The qualitative orbital interaction diagram which gives the splitting of the s, d and p valence orbitals of a transition metal with the electron configuration $(n)s^0(n-1)d^6$ and the electronic reference state t_{2g} in the octahedral field of ligands which have σ and π orbitals is shown in Fig. 4. The results of the ETS analysis are given in Table 2.

The DCD model suggests for the orbital interactions between $TM^q(t_{2g})$ and $(CO)_6$ that there should be $TM^q \leftarrow (CO)_6$ σ donation arising from orbitals which have a_{1g}, t_{1u} and e_g symmetry and that the $TM^q \rightarrow (CO)_6$ π backdonation should come from orbitals which have t_{2g} symmetry. Fig. 4 shows that the metal s, d and p valence orbitals which may interact with $(CO)_6$ through σ donation belong to the a_{1g}, t_{1u} and e_g sets. This means that the strengths of the σ orbital interactions having the above symmetry give the relative importance of the TM valence AOs directly. This is an important side result of the ETS analysis. The question whether the empty metal (n)p orbitals should be considered as true valence orbitals or as polarisation functions like the empty d orbitals in the chemistry of heavier main group elements has been the topic of a controversial discussion [34]. The calculated values of the ΔE_{orb} term will give important information about this point.

Table 2 shows that the calculated interactions energies ΔE_{int} have again a U-shaped trend but the lowest value is found for $Re(CO)_6^+$ which is slightly lower than for $W(CO)_6$ [50]. The trend of the energy terms is graphically shown in Fig. 5. The Pauli repulsion increases from $Hf(CO)_6^{2-}$ to $Re(CO)_6^+$ but then it decreases up to $Ir(CO)_6^{3+}$. Although the trend of the ΔE_{Pauli} term agrees qualitatively with the trend of ΔE_{int} it does not show the large changes which are found for the interaction energy when one goes from $Re(CO)_6^+$ to $Ir(CO)_6^{3+}$. Note that the electrostatic interactions change very little along the hexacarbonyls and that the highest charged species $Hf(CO)_6^{2-}$ and $Ir(CO)_6^{3+}$ have the lowest ΔE_{elstat} values. The very large interaction energies of $Os(CO)_6^{2+}$ and particularly $Ir(CO)_6^{3+}$ correlate nicely with the large increase of the ΔE_{orb} values, however. Table 2 and Fig. 5 show that the very strong attraction between the metal cations Os^{2+} and Ir^{3+} and the $(CO)_6$ ligand cage is mainly caused by the strong increase of the orbital interactions. Yet, the trend of the ΔE_{orb} values does not completely agree with the ΔE_{int} values. $Re(CO)_6^+$ has a smaller ΔE_{int} value than $W(CO)_6$ although the ΔE_{orb} value of the latter is lower (Table 2).

Inspection of the different orbital contributions to the ΔE_{orb} term shows that the t_{2g} energy values, which give the $TM^q \rightarrow (CO)_6$ π backdonation are the largest ones for $W(CO)_6$ and for the negatively charged complexes. The e_g interactions which give the $TM^q \leftarrow (CO)_6$ σ donation into the d(σ) metal orbitals (Fig. 4) become the dominant contributor in the positively charged species. The orbital contributions to the $TM^q \leftarrow (CO)_6$ σ donation into the s and p valence orbitals of the metal which are given by the a_{1g} and t_{1u} orbitals (Fig. 4) are

much smaller than the e_g values. This means that the d valence orbitals of the metals are much more important as acceptor orbitals than the s and p orbitals. However, the energy values of the t_{1u} orbitals are always larger than the a_{1g} values (Table 2). This means that the p orbitals should be considered as true valence orbitals and not only as polarisation functions.

The orbital interactions which have t_{1u} symmetry are actually more complicated than shown in Fig. 4. Fig. 6 shows a schematic representation of all orbitals contributing to the ΔE_{orb} term that have been found by the ETS analysis. The t_{1u} term comprises two different types of $TM^q \leftarrow (CO)_6$ donation, i.e. σ donation from the lone-pair σ orbitals of $(CO)_6$ and π donation from the occupied π orbitals of the ligand cage. The latter interaction is often neglected in qualitative discussions of metal–ligand bonding but it has been suggested that it could play a role in carbonyl complexes [35]. The ETS analysis cannot distinguish between these σ and π donations because both have t_{1u} symmetry. An estimate of the σ and π components of the t_{1u} interactions using the orbital overlaps led to the values which are given in the last two lines of Table 2 [20]. The data suggest that the π component is always much weaker than the σ component.

Fig. 6 also shows the t_{1g} and t_{2u} orbitals which according to the ETS analysis make small contributions to ΔE_{orb} although they are not found in the orbital correlation diagram shown in Fig. 4. They are pure ligand orbitals because there is no metal AO which has t_{1g} or t_{2u} symmetry. The small energy contributions come from the relaxation of the valence orbitals in the final step of the ETS analysis. Thus, the energy values of the ΔE_{orb} term arise not only from interatomic bonding interactions but also from the relaxation of the fragment orbitals. However, this effect is relatively small.

As a summary it can be said that the qualitative bonding models which are shown in Figs. 1 and 4 are complemented by the quantitative data which are given in Tables 1 and 2. The results also give a more complete picture of the nature of the metal–CO bonding in neutral and charged carbonyl complexes which is based on a physical interpretation of the electronic structure.

4. Complexes with Group-13 diyl ligands $(CO)_4Fe$–ER (E = B, Al, Ga, In, Tl; R = Cp, Ph) [21]

While carbonyls were the first TM complexes which have been synthesised [36], molecules with Group-13 ligands ER (E = Group-13 element B-Tl) belong to the youngest classes of TM complexes. The first TM Group-13 diyl complex characterised by X-ray structure analysis which is not stabilised by additional donor ligands is $(CO)_4Fe$–AlCp* which has been reported by Weiss et al. in 1997 [37]. The first homoleptical diyl complex $Ni(InC(SiMe_3)_3)_4$ was synthesised by Uhl et al. in 1998 [38]. The DCD model of the TM–ER bonding is shown in Fig. 7.

A comparison of the donor–acceptor models for TM–CO bonding (Fig. 1) with TM–ER bonding (Fig. 7) suggests that the bonding situation should be similar. The pivotal difference concerns the strength of the TM → ER π backdonation. The p(π) orbitals of atom E receives electronic charge from the π orbitals of R and from the d(π) orbitals of E. Ligands R which are poor π donors should lead to stronger TM → ER π backdonation. The first TM complexes with ER ligands which could be isolated have strong π-donor groups R such as Cp* [37,49] and $N(SiMe_3)_2$ [39]. This led initially to the idea that Group-13 diyl complexes might only be stable when R is a good π-donor. However, later work showed that complexes where R is a poor donor can also become isolated [40]. The syntheses and X-ray

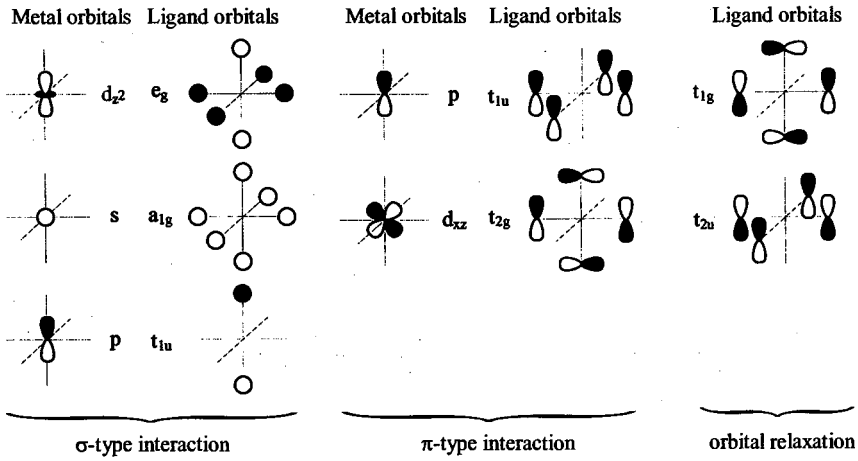

Fig. 6. Schematic representation of the orbitals with different symmetry which contribute to the ΔE_{orb} term according to the ETS analysis of $TMq–(CO)_6$ (Table 2). Reproduced with permission from Ref. [20].

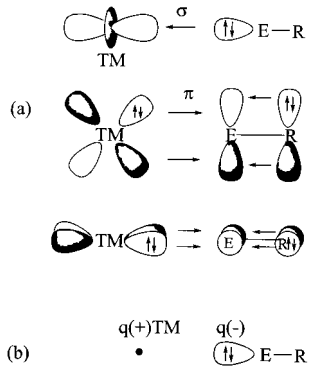

Fig. 7. (a) Schematic representation of the TM–ER orbital interactions when R has occupied p(π) orbitals. (b) Schematic representation of the dominant electrostatic interactions between the local electronic charge concentration at the donor atom E and the nucleus of the acceptor atom Fe. Note that the donor atom E has an overall positive partial charge and the Fe atom an overall negative partial charge.

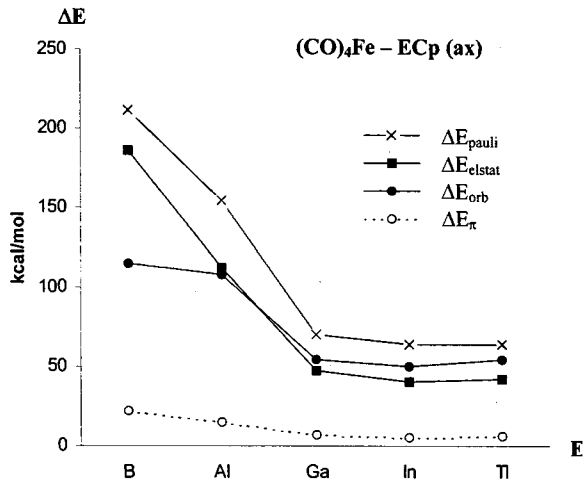

Fig. 8. Absolute values of the energy contributions of the Pauli repulsion ΔE_{Pauli}, electrostatic interactions ΔE_{elstat}, total orbital interactions ΔE_{orb} and π-orbital interactions ΔE_{π} to the Fe–E bonding interactions in the axial form of $(CO)_4$Fe–ECp. Reproduced with permission from Ref. [21].

structure analyses of the homoleptical complexes $Ni(EC(SiMe_3)_3)_4$ with E = In [38] and E = Ga [41] and the surprising stability of $(CO)_4$Fe–GaAr* (Ar* = 2,6-(2,4,6-triisopropylphenyl)phenyl) [42] showed that sterically crowded ligands ER which have poor π-donor groups R are stable in a condensed phase. The rather short Fe–Ga interatomic distance in the latter complex led to the suggestion that there is strong Fe→Ga π backdonation and therefore, the Fe–Ga bond order is three [42]. This has been questioned in two theoretical analyses of the electronic charge distribution which showed that the Fe→Ga π-donation is rather low [43,44].

The question about the bonding situation in TM Group-13 diyl complexes has been studied by us in a detailed energy analysis of the compounds $(CO)_4$FeER, $Fe(EMe)_5$ and $Ni(EMe)_4$ with E = B–Tl and R = Cp, $N(SiH_3)_2$, Ph and Me [21]. Both axial and equatorial isomers of $(CO)_4$FeER have been considered. Here we present the most relevant results of $(CO)_4$FeER with the strong π donor group R = Cp and with the weak π donor R = phenyl. We also discuss the results which were obtained for $Fe(EMe)_5$ and $Ni(EMe)_4$.

Table 3 shows the ETS results for the axial forms of $(CO)_4$FeECp. The equatorial form of E = B is not a minimum on the PES [21]. The equatorial isomers of the other elements are slightly (< 2 kcal mol^{-1}) lower in energy than the axial form except for the indium complex. The equatorial form of $(CO)_4$FeInCp is predicted to be 0.2 kcal mol^{-1} more stable than the axial form [21]. Since the ETS results of the axial and equatorial isomers were found to be very similar we discuss only the data of the axial form. The results for $Fe(CO)_5$ are given for comparison. Fig. 8 gives schematically the trend of the energy components ΔE_{Pauli}, ΔE_{elstat} and ΔE_{orb} and the π contribution to the latter term ΔE_{π}.

Table 3
ETS analysis of the axial isomers of $Fe(CO)_4$–ECp and $Fe(CO)_5$ (kcal mol^{-1}); calculated bond distances Fe–E (Å) [a]

	BCp	AlCp	GaCp	InCp	TlCp	CO
ΔE	−75.3	−52.7	−23.0	−19.8	−13.6	−46.5
ΔE_{prep}	15.0	12.5	8.7	7.3	19.5	8.1
ΔE_{int}	−90.3	−65.2	−31.7	−27.1	−33.1	−54.6
ΔE_{Pauli}	211.6	154.3	69.8	63.6	64.1	134.8
ΔE_{elstat} [b]	−186.0 (61.6%)	−112.1 (51.1%)	−47.1 (46.6%)	−40.0 (44.1%)	−42.7 (44.0%)	−98.0 (51.7%)
ΔE_{orb} [b]	−115.9 (38.4%)	−107.4 (48.9%)	−54.4 (53.4%)	−50.7 (55.9%)	−54.2 (56.0%)	−91.4 (48.3%)
ΔE_{σ} [c]	−93.8 (80.9%)	−92.3 (85.9%)	−47.2 (86.8%)	−45.3 (89.3%)	−48.9 (89.4%)	−47.6 (52.1%)
ΔE_{π} [c]	−22.1 (19.1%)	−15.1 (14.1%)	−7.2 (13.2%)	−5.4 (10.7%)	−5.8 (10.6%)	−43.8 (47.9%)
Distances						
Fe–E	1.968	2.253	2.395	2.548	2.578	

[a] Values taken from Ref. [21].
[b] Values in parentheses give the percentage contribution to the total attractive interactions $\Delta E_{\text{elstat}} + \Delta E_{\text{orb}}$.
[c] Values in parentheses give the percentage contribution to the total orbital interactions ΔE_{orb}.

The bond dissociation energies ΔE ($= -D_e$) which are given in the last line of Table 3 suggest that the bond strength of the Fe–ECp bond has the order for E = B > Al > Ga > In > Tl. The preparation energies which give the deformation of the fragments $Fe(CO)_4$ and ECp are in most cases small. Thus, the interaction energies ΔE_{int} show the same trend as ΔE except for E = Tl. The thallium complex has a comparatively large interaction energy but also a large preparation energy which makes $(CO)_4$FeTlCp the weakest bonded complex in the series. Indeed, there is no thallium diyl complex which could become isolated until now.

Table 3 shows that the Fe–ER bonds of the heavier elements E = Al–Tl are predicted to be ca. half ionic and ca. half covalent. It is interesting to note that the Fe–CO bond has a similar ratio of ΔE_{elstat} and ΔE_{orb} as the heavier diyl complexes. The borylene complex $(CO)_4$Fe–BCp, however, has a significantly less covalent and more ionic bond than the heavier analogues. This has been explained with the σ orbital interactions at short Fe–ER distances. The results given in Table 3 show that the dominant contributions to ΔE_{orb} come from σ interactions. Fig. 7 shows that the σ-donor orbital of E at first overlaps in a bonding fashion with the lope of the d_{z2} acceptor orbital of TM which has the same sign. However, at shorter distances there is an overlap with the tubular-shaped lope of the d_{z2} orbital which has an opposite sign, leading to antibonding interactions with the σ-donor orbital. This effect should become important when the donor and acceptor atoms come closer to each other. Boron has clearly the shortest equilibrium distance of the TM–E bonds (first line in Table 3). The electrostatic interactions do not depend on the sign of the occupied orbitals that contribute to the ΔE_{elstat} term. Fig. 7b shows that the electrostatic attraction between the donor atom E and the acceptor atom TM depends mainly on the interatomic distance. The borylene complex has clearly the shortest Fe–B bond lengths and thus, has the highest ΔE_{elstat} value. Fig. 8 shows that the three energy terms ΔE_{Pauli}, ΔE_{elstat} and ΔE_{orb} run parallel from the right (Tl) to the left (Al) but the ΔE_{orb} contribution of boron remains nearly the same as for aluminium while the other two terms sharply increase.

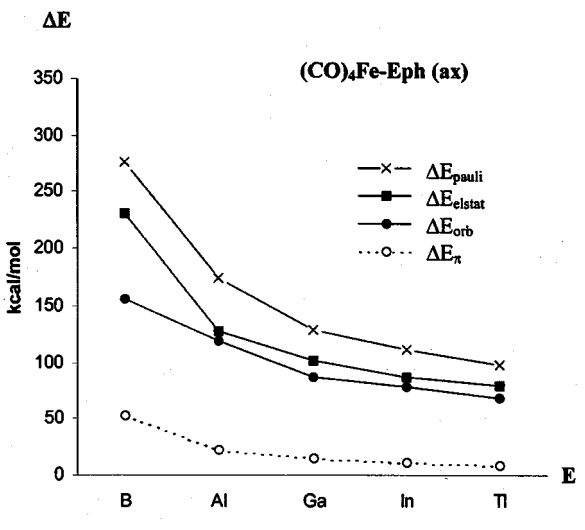

Fig. 9. Absolute values of the energy contributions of the Pauli repulsion ΔE_{Pauli}, electrostatic interactions ΔE_{elstat}, total orbital interactions ΔE_{orb} and π-orbital interactions ΔE_{π} to the Fe–E bonding interactions in the axial form of $(CO)_4$Fe–EPh. Reproduced with permission from Ref. [21].

Table 3 and Fig. 8 show that the energy contributions of the π orbitals to the interaction energies of the Fe–ECp bond are rather small. The largest relative contribution is found for the boron complex (19.1% of ΔE_{orb}) and the smallest for the thallium complex (10.6%). Note that the π-contribution of the Fe–CO bond (47.9%) is much higher than those of the Fe–ECp bonds. The Fe–CO bond of $Fe(CO)_5$ has a comparable interaction energy as the $(CO)_4$Fe–AlCp bond and the contributions of the energy components ΔE_{Pauli}, ΔE_{elstat} and ΔE_{orb} in the two bonds are similar. It is only the π-bonding which clearly distinguishes the nature of the Fe–CO and Fe–AlCp bonds.

Table 4 gives the results of the ETS analysis of $(CO)_4$Fe–EPh. The trend of the energy terms of the axial isomers is shown in Fig. 9. The interatomic distances of the Fe–EPh bonds are always shorter than those of the Fe–ECp bonds (Table 3) and the bond energies ΔE and interaction energies ΔE_{int} of the former are larger than those of the latter. The trend of the energy components ΔE_{Pauli}, ΔE_{elstat} and ΔE_{orb} of the two series of complexes is similar (Figs. 8 and 9). The heavier EPh complexes with E = Al–Tl have, like the ECp complexes, a higher covalent character than the boron complex. The pivotal question concerns the π orbital contributions to ΔE_{orb}. Table 4 shows that the ΔE_{π} values of the EPh complexes are higher than the values of the ECp complexes which are given in Table 3, but the π contribution is still significantly less than the σ contribution. The highest ΔE_{π} value is found for the boron complex where the π contribution is ca. one-third of the covalent bonding. The model compound $(CO)_4$Fe–GaPh of the gallium aryl complex $(CO)_4$Fe–GaPh* which was claimed to have a triple bond [42] has only 17.2% π-bonding contribution in the more stable axial form.

Table 4 also gives the results of the slightly (< 3 kcal mol^{-1}) [21] less stable equatorial forms of $(CO)_4$Fe–EPh because the C_{2v} symmetry of the latter makes it possible to distinguish between the nondegenerate Fe–EPh π bonding contributions to ΔE_{orb}. The π orbitals with b_1 symmetry give the π energy contributions which are in the phenyl plane while the π orbitals with b_2 symmetry give the π energy contributions which are orthogonal to the phenyl plane. Table 4 shows that

Table 4
ETS analysis of the axial and equatorial isomers of $Fe(CO)_4$–EPh (kcal mol^{-1}) and calculated interatomic distances TM–E (Å) [a]

	BPh		AlPh		GaPh		InPh		TlPh	
	Ax	Eq	Ax	Eq	Ax	Eq	Ax	Eq	Ax	Eq
ΔE	−100.2	−99.0	−63.8	−62.9	−52.3	−49.4	−40.7	−43.5	−40.8	−38.0
ΔE_{prep}	10.1	10.8	9.4	8.2	8.7	6.1	8.1	5.2	8.6	4.9
ΔE_{int}	−110.3	−109.8	−73.2	−71.1	−61.0	−55.5	−48.8	−48.7	−49.4	−42.9
ΔE_{Pauli}	276.6	319.2	173.8	192.3	129.5	130.0	112.3	112.2	98.7	96.4
ΔE_{elstat} [b]	−230.4 (59.6%)	−258.8 (60.3%)	−127.3 (51.5%)	−147.6 (56.0%)	−102.3 (53.7%)	−107.5 (58.0%)	−87.0 (54.0%)	−91.7(57.0%)	−79.3 (53.5%)	−81.3 (58.6%)
ΔE_{orb} [b]	−156.5 (40.4%)	−170.2 (39.7%)	−119.7 (48.5%)	−115.8 (44.0%)	−88.2 (46.3%)	−76.0 (42.0%)	−74.1 (46.0%)	−69.2 (43.0%)	−68.8 (46.5%)	−58.0 (41.4%)
ΔE_{σ} [c]	−104.3 (66.6%)	−110.3 (64.8%)	−98.2 (82.0%)	−91.6 (79.1%)	−73.0 (82.8%)	−61.7 (79.1%)	−63.4 (85.6%)	−57.7 (83.4%)	−59.8 (86.9%)	−48.6 (83.8%)
ΔE_{π} [c]	−52.2 (33.4%)	−59.9 (35.2%)	−21.5 (18.0%)	−24.2 (20.9%)	−15.2 (17.2%)	−16.3 (20.9%)	−10.7 (14.4%)	−11.5 (16.6%)	−9.0 (13.1%)	−9.4 (16.2%)
$\Delta E_{\pi(b1)}$ [d]	–	−39.3	–	−15.6	–	−11.4	–	−8.2	–	−6.7
$\Delta E_{\pi(b2)}$ [d]	–	−20.7	–	−8.6	–	−4.9	–	−3.3	–	−2.7
Distances										
TM–E	1.803	1.800	2.217	2.206	2.296	2.304	2.478	2.488	2.478	2.544

[a] Values taken from Ref. [21].
[b] Values in parentheses give the percentage of the attractive interactions $\Delta E_{elstat} + \Delta E_{orb}$.
[c] Values in parentheses give the percentage contribution to the total orbital interactions ΔE_{orb}.
[d] π(b1)-orbital is in the Ph plane and π(b2)-orbital is perpendicular to the Ph plane.

Table 5
ETS analysis of the equatorial Fe–E bonds of the complexes $Fe(ECH_3)_5$ (kcal mol^{-1}) and calculated interatomic distances TM–E (Å) [a]

	BCH_3	$AlCH_3$	$GaCH_3$	$InCH_3$	$TlCH_3$
ΔE	−105.6	−79.2	−64.1	−57.4	−53.1
ΔE_{prep}	13.6	7.8	2.9	2.1	1.1
ΔE_{int}	−119.2	−87.0	−67.0	−59.5	−54.1
ΔE_{pauli}	247.8	140.2	120.8	113.9	113.0
ΔE_{elstat} [b]	−228.4 (62.2%)	−135.4 (59.6%)	−115.2 (61.3%)	−107.8 (62.2%)	−103.8 (62.1%)
ΔE_{orb} [b]	−138.6 (37.8%)	−91.8 (40.4%)	−72.6 (38.7%)	−65.6 (37.8%)	−63.3 (37.9%)
ΔE_{σ} [c]	−74.6 (53.8%)	−55.0 (59.9%)	−45.5 (62.7%)	−41.7 (63.6%)	−42.9 (67.8%)
ΔE_{π} [c]	−64.0 (46.2%)	−36.8 (40.1%)	−27.1 (37.3%)	−23.9 (36.4%)	−20.4 (32.2%)
Distances					
TM–E	1.772	2.174	2.255	2.434	2.474

[a] Values taken from Ref. [21].
[b] Values in parentheses give the percentage of attractive interactions $\Delta E_{elstat} + \Delta E_{orb}$.
[c] Values in parentheses give the percentage contribution to the total orbital interactions ΔE_{orb}.

the $\Delta E_{\pi(b1)}$ values are ca. twice as high as the $\Delta E_{\pi(b2)}$ values. This is reasonable because the b_2 π electrons compete with the π electrons of the phenyl ring while there is no such competition for the b_1 electrons.

The ETS results of the complexes $(CO)_4FeER$ have shown that the contribution of the Fe→ER π backdonation to the bonding interactions is much smaller than the Fe←ER σ donation even when R is a poor π donor. The question which was also addressed by us is whether the bonding situation changes significantly when the ER ligand does not compete with a strong π acceptor like CO in $(CO)_4FeER$ [21]. To this end we carried out ETS analyses of the homoleptical complexes $Fe(EMe)_5$. We also investigated the bonding situation in the nickel complexes $Ni(EMe)_4$ in order to find out if the bonding situation becomes different when TM is a later transition metal. Table 5 gives the ETS results of $Fe(EMe)_5$. The trend of the energy terms is shown in Fig. 10.

The following conclusions can be drawn from the data which are given in Table 5. The Fe–E bonds of the homoleptical complexes are stronger than the Fe–E bonds of the carbonyl complexes $(CO)_4Fe$–E [45]. The calculated ΔE_{elstat} and ΔE_{orb} values suggest that the Fe–E bonds in the homoleptic complexes are more ionic and less covalent than in the carbonyl complexes. Another difference is that the covalent contribution to the bonding in the homoleptic complexes remains nearly the same for all elements E = B–Tl. The largest difference in the nature of the Fe–E between the $Fe(EMe)_5$ species and the $(CO)_4FeER$ complexes was found for the π contribution. Table 5 shows that the ΔE_{π} values are between 32 (E = Tl) and 46% (E = B) of the total ΔE_{orb} values. Thus, π bonding makes a significant contribution to the covalent Fe–EMe bonding in complexes where there is no competition with other strong π accepting ligands.

Table 6 and Fig. 11 show the ETS results of the homoleptical nickel complexes $Ni(EMe)_4$. A comparison with the data of the homoleptical iron complexes shows that the TM–EMe bonds of the nickel complexes have a larger ionic character than the iron species. The π bonding contribution of the Ni complexes is a bit higher than in the Fe complexes.

The ETS results of the Group-13 diyl complexes give an answer to the controversy about the strength of the π bonding in the gallium complex $(CO)_4Fe$–GaAr* but also the data give a deep insight into the nature of the bonding in terms of ionic versus covalent bonding. The results explain the difference between Fe–ER and Fe–CO bonds and they rationalise the influence of the substituent R on the Fe–ER bonding and they lead to an understanding of the differences among the Group-13 elements B–Tl.

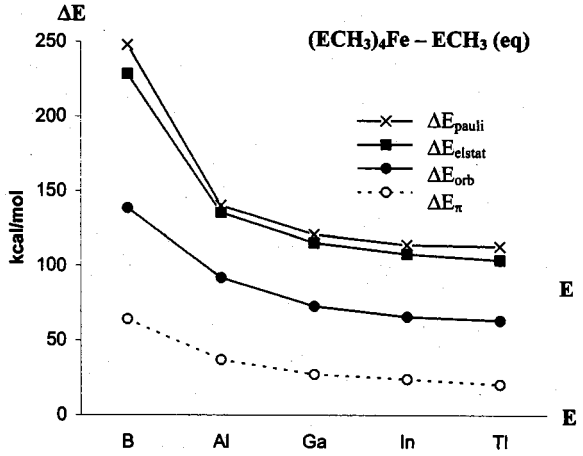

Fig. 10. Absolute values of the energy contributions of the Pauli repulsion ΔE_{Pauli}, electrostatic interactions ΔE_{elstat}, total orbital interactions ΔE_{orb} and π-orbital interactions ΔE_{π} to the Fe–E (equatorial) bonding interactions in $Fe(EMe)_5$. Reproduced with permission from Ref. [21].

Table 6
ETS analysis of the complexes $Ni(ECH_3)_4$ (kcal mol^{-1}) and calculated interatomic distances TM–E (Å) [a]

	BCH_3	$AlCH_3$	$GaCH_3$	$InCH_3$	$TlCH_3$
ΔE	−92.3	−61.6	−46.6	−40.7	−35.7
ΔE_{prep}	3.4	3.1	3.5	3.2	5.1
ΔE_{int}	−95.7	−64.7	−50.1	−43.9	−40.8
ΔE_{pauli}	236.8	131.5	113.6	105.8	103.7
ΔE_{elstat} [b]	−215.9 (64.9%)	−123.2 (62.8%)	−107.3 (65.5%)	−99.8 (66.7%)	−96.1 (66.4%)
ΔE_{orb} [b]	−116.6 (35.1%)	−73.0 (37.2%)	−56.4 (34.5%)	−49.9 (33.3%)	−48.4 (33.6%)
ΔE_{σ} [c]	−60.0 (51.5%)	−45.3 (62.1%)	−33.9 (60.1%)	−30.5 (61.1%)	−31.2 (64.5%)
ΔE_{π} [c]	−56.6 (48.5%)	−27.7 (37.9%)	−22.5 (39.9%)	−19.4 (38.9%)	−17.2 (35.5%)
Distances					
TM–E	1.769	2.165	2.238	2.399	2.447

[a] Values taken from Ref. [21].
[b] Values in parentheses give the percentage of the attractive interactions $\Delta E_{elstat} + \Delta E_{orb}$.
[c] Values in parentheses give the percentage contribution to the total orbital interactions ΔE_{orb}.

5. Complexes with cyclic π-donor ligands $Fe(Cp)_2$ and $Fe(\eta^5\text{-}N_5)_2$ [22]

In the final paragraph we compare the results of an ETS analysis of ferrocene with the data of the isoelectronic iron bispentazole. The former compound was already synthesised in 1951 [46]. Soon after the sandwich structure of $Fe(Cp)_2$ was recognised [47] the metal–ligand bonding was discussed in terms of the DCD donor–acceptor interactions between Fe^{2+} and 2 Cp^- shown in Fig. 12. Although the cyclopentadienyl ligands of ferrocene in the gas phase are eclipsed it has been found reasonable to discuss the orbital interactions in D_{5d} symmetry (staggered ligands) rather than using D_{5h} symmetry [8,10].

The isoelectronic bispentazole complex $Fe(\eta^5\text{-}N_5)_2$ is experimentally not yet known. In a recent paper we predicted that $Fe(\eta^5\text{-}N_5)_2$ is a strongly bonded molecule which has a total bond energy for dissociation into $Fe + 2$ cyc-N_5 $D_o = 109$ kcal mol^{-1} which is only ca. 30 kcal mol^{-1} less than the BDE of ferrocene [22]. Although iron bispentazole is a high-energy compound which is thermodynamically unstable [48] toward dissociation into $Fe + 5N_2$ it should be possible to synthesise it. The equilibrium geometry of $Fe(\eta^5\text{-}N_5)_2$ has D_{5d} symmetry, i.e. the cyc-N_5 rings are staggered [22]. The results of the ETS analyses of ferrocene and iron bispentazol are given in Table 7.

The calculated interaction energies ΔE_{int} between $Fe^{2+}(t_{2g}^6)$ and 2 L^- (L = Cp, cyc-N_5) are very large. The high energy values come by the strong electrostatic attraction between the doubly positively charged iron and the negatively charged L^- ligands. Table 7 shows that the orbital contributions and the electrostatic contributions have about the same strength in both complexes. Thus, the iron–ligand bonding in $Fe(Cp)_2$ and

Table 7
ETS analysis of $Fe(Cp)_2$ and $Fe(N_5)_2$ (kcal mol^{-1}) [a]

Term	$Fe(C_5H_5)_2$	$Fe(N_5)_2$
ΔE_{int} [b]	−893.3	−706.7
ΔE_{Pauli}	272.2	244.0
ΔE_{elstat} [c]	−598.0 (51.3%)	−492.6 (51.8%)
ΔE_{orb} [c]	−567.5 (48.7%)	−458.1 (48.2%)
A_{1g} [d]	−48.5 (8.5%)	−40.6 (8.9%)
A_{2g}	0.0	0.0
E_{1g} [d]	−367.2 (64.7%)	−285.4 (62.3%)
E_{2g} [d]	−46.1 (8.1%)	−44.7 (9.8%)
A_{1u}	0.0	0.0
A_{2u} [d]	−28.2 (5.0%)	−22.3 (4.9%)
E_{1u} [d]	−61.1 (10.8%)	−44.5 (9.7%)
E_{2u} [d]	−16.4 (2.9%)	−20.6 (4.5%)

[a] Values taken from Ref. [22].
[b] Fe^{2+} $(t_{2g}^6) + 2L^-$.
[c] Values in parentheses give percentage of the attractive interactions $\Delta E_{elstat} + \Delta E_{orb}$.
[d] Values in parentheses give percentage of orbital interactions ΔE_{orb}.

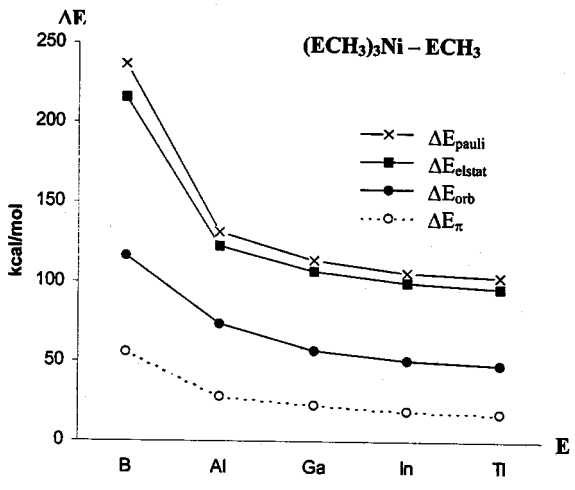

Fig. 11. Absolute values of the energy contributions of the Pauli repulsion ΔE_{Pauli}, electrostatic interactions ΔE_{elstat}, total orbital interactions ΔE_{orb} and π-orbital interactions ΔE_{π} to the Ni–E bonding interactions in $Ni(EMe)_4$. Reproduced with permission from Ref. [21].

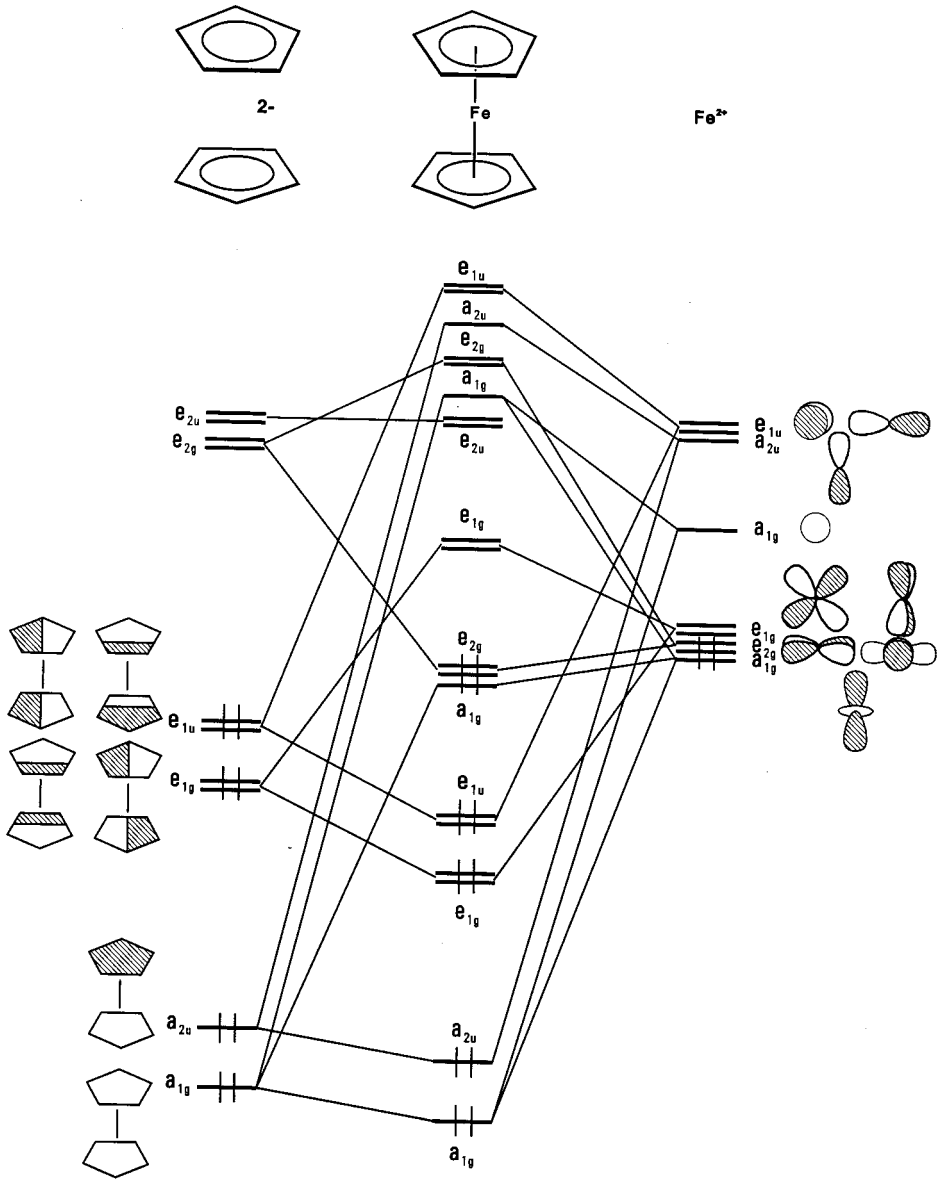

Fig. 12. MO correlation diagram of the interactions between Fe^{2+} and a five-membered cyclic ligand X_5^- (X = CH, N).

$Fe(\eta^5\text{-}N_5)_2$ is about half ionic and half covalent. The covalent contributions come mainly from the orbitals which have e_{1g} symmetry. Fig. 13 shows the e_{1g} orbitals of ferrocene and $Fe(\eta^5\text{-}N_5)_2$. It is obvious that the orbital contributions come from the $Fe^{2+} \leftarrow (L^-)_2$ π donation which give 64.7 ($L^- = Cp^-$) and 62.3% ($L^- = \eta^5\text{-}N_5$) to the ΔE_{orb} term. The remaining contributions are less important. It is remarkable that the nature of the bonding in ferrocene and in the experimentally yet unknown iron bispentazole is nearly identical.

6. Summary

The discussion of the results which have been obtained for three different classes of TM complexes demonstrate how much progress has been made in the development of methods which give insight into the nature of the metal–ligand bonding situation. The molecular orbital model suggested by Dewar 50 years ago which has become a standard model for a qualitative understanding of the structure and bonding of TM compounds is quantitatively supported by the ETS results. However, the picture which emerges from the ETS analysis is far more complete and it does not leave room for speculations about the strength of the σ and π contributions to the bonding. Moreover it shows that the electrostatic contribution to the bonding and the Pauli repulsion need to be considered in order to give a full understanding of the nature of the chemical bond. It is possible to give accurate geometries, bond energies, vibrational frequencies and other properties of TM

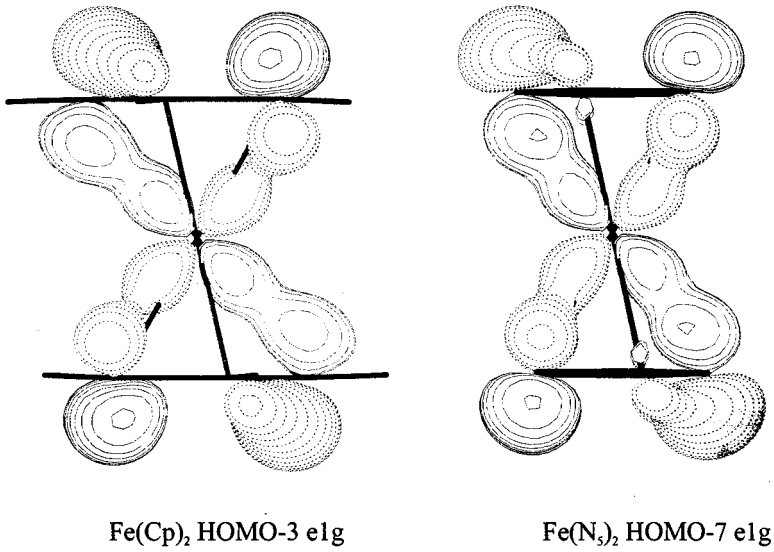

Fig. 13. Plot of the (e_{1g}) Kohn–Sham orbitals of ferrocene and iron bispentazole which make the largest contribution to the orbital interaction term ΔE_{orb}. Reproduced with permission from Ref. [22].

complexes. Quantum chemical methods can also be used to give a detailed picture of the bonding situation which is based on accurate calculations and well defined partitioning procedures.

Acknowledgements

This work was supported by the Deutsche Forschungsgemeinschaft and by the Fonds der Chemischen Industrie. Excellent service by the Hochschulrechenzentrum of the Philipps-Universität Marburg is gratefully acknowledged. Additional computer time was provided by the HLRS Stuttgart, HHLRZ Darmstadt and HRZ Frankfurt.

References

[1] A. Kekulé, Bull. Soc. Chim. Fr. 3 (1965) 98.
[2] E. Hückel, Z. Phys. 70 (1931) 204.
[3] V.I. Minkin, M.N. Glukhovtsev, B.Ya. Simkin, Aromaticity and Antiaromaticity, Wiley, New York, 1994.
[4] (a) R.B. Woodward, R. Hoffmann, The Conservation of Orbital Symmetry, Verlag Chemie, Weinheim, 1970;
(b) K Fukui, Acc. Chem. Res. 4 (1971) 57.
[5] I. Fleming, Frontier Orbitals and Organic Chemical Reactions, Wiley, New York, 1976.
[6] M.J.S. Dewar, Bull. Soc. Chim. Fr. 18 (1951) C79.
[7] J. Chatt, L.A. Duncanson, J. Chem. Soc. (1953) 2929.
[8] (a) F.A. Cotton, G. Wilkinson, C.A. Murillo, M. Bochmann, Advanced Inorganic Chemistry, 6th ed., Wiley, New York, 1999;
(b) D.F. Shriver, P.W. Atkins, C.H. Langford, Inorganic Chemistry, 2nd ed., Oxford University Press, Oxford, 1994;
(c) J.E. Huheey, E.A. Keiter, R.L. Keiter, Inorganic Chemistry: Principles of Structure and Reactivity, 4th ed., Benjamin/Cummings, New York, 1993;
(d) Ch. Elschenbroich, A. Salzer, Organometallics, 2nd ed., VCH, Weinheim, 1992.
[9] Representative examples: (a) R. Hoffmann, M.M.L. Chen, D.L. Thorn, Inorg. Chem. 16 (1977) 503;
(b) B.E.R. Schilling, R. Hoffmann, J. Am. Chem. Soc. 101 (1979) 3456;
(c) R. Hoffmann, Science 211 (1981) 995;
(d) R. Hoffmann, T.A. Albright, D.L. Thorn, Pure Appl. Chem. 50 (1978) 1;
(e) Y. Jean, A. Lledos, J.K. Burdett, R. Hoffmann, J. Am. Chem. Soc. 110 (1988) 4506.
[10] T.A. Albright, J.K. Burdett, M.H. Whangbo, Orbital Interactions in Chemistry, Wiley, New York, 1985.
[11] M. Diedenhofen, T. Wagener, G. Frenking, in: T.R. Cundari (Ed.), Computational Organometallic Chemistry, Marcel Dekker, New York, 2001, p. 69.
[12] A.E. Reed, L.A. Curtiss, F. Weinhold, Chem. Rev. 88 (1988) 899.
[13] R.F.W. Bader, Atoms in Molecules: a Quantum Theory, Oxford University Press, Oxford, 1990.
[14] S. Dapprich, G. Frenking, J. Phys. Chem. 99 (1995) 9352.
[15] (a) G. Frenking, U. Pidun, J. Chem. Soc. Dalton Trans. (1997) 1653;
(b) U. Pidun, G. Frenking, J. Organomet. Chem. 525 (1996) 269;
(c) U. Pidun, G. Frenking, Organometallics 14 (1995) 5325;
(d) S.F. Vyboishchikov, G. Frenking, Chem. Eur. J. 4 (1998) 1428;
(e) A.W. Ehlers, S. Dapprich, S.F. Vyboishchikov, G. Frenking, Organometallics 15 (1996) 105;
(f) S. Dapprich, G. Frenking, Organometallics 15 (1996) 4547;
(g) G. Frenking, S. Dapprich, K.F. Köhler, W. Koch, J.R. Collins, Mol. Phys. 89 (1996) 1245;
(h) S. Dapprich, G. Frenking, Angew. Chem. 107 (1995) 383 (Angew. Chem. Int. Ed. Engl. 34 (1995) 354);
(i) S. Fau, G. Frenking, Mol. Phys. 96 (1999) 519.
[16] (a) T. Ziegler, A. Rauk, Theor. Chim. Acta 46 (1977) 1;
(b) T. Ziegler, A. Rauk, Inorg. Chem. 18 (1979) 1558;
(c) T. Ziegler, A. Rauk, Inorg. Chem. 18 (1979) 1755.
[17] K. Morokuma, Acc. Chem. Res. 10 (1977) 294.
[18] E.R. Davidson, K.L. Kunze, F.B.C. Machado, S.J. Chakravorty, Acc. Chem. Res. 26 (1993) 628.
[19] Y. Chen, G. Frenking, J. Chem. Soc. Dalton Trans. (2001) 434.

[20] A. Diefenbach, F.M. Bickelhaupt, J. Am. Chem. Soc. 122 (2000) 6449.
[21] J. Uddin, G. Frenking, J. Am. Chem. Soc. 123 (2001) 1683.
[22] M. Lein, J. Frunzke, A. Timoshkin, G. Frenking, Chem. Eur. J., in press.
[23] N. Fröhlich, G. Frenking, Chem. Rev. 100 (2000) 717.
[24] A.D. Becke, Phys. Rev. A 38 (1988) 3098.
[25] J.P. Perdew, Phys. Rev. B 33 (1986) 8822.
[26] (a) C. Chang, M. Pelissier, Ph. Durand, Phys. Scr. 34 (1986) 394; (b) J.-L. Heully, I. Lindgren, E. Lindroth, S. Lundquist, A.-M. Martensson-Pendrill, J. Phys. B 19 (1986) 2799; (c) E. van Lenthe, E.J. Baerends, J.G. Snijders, J. Chem. Phys. 99 (1993) 4597; (d) E. van Lenthe, E.J. Baerends, J.G. Snijders, J. Chem. Phys. 105 (1996) 6505; (e) E. van Lenthe, R. van Leeuwen, E.J. Baerends, J.G. Snijders, Int. J. Quantum Chem. 57 (1996) 281.
[27] (a) J.G. Snijders, Mol. Phys. 36 (1978) 1789; (b) J.G. Snijders, P. Ross, Mol. Phys. 38 (1979) 1909.
[28] J.G. Snijders, E.J. Baerends, P. Vernooijs, Atm. Nucl. Data Tables 26 (1982) 483.
[29] E.J. Baerends, D.E. Ellis, P. Ros, Chem. Phys. 2 (1973) 41.
[30] J. Krijn, E.J. Baerends, Fit Functions in the HFS-Method, Internal Report (in Dutch), Vrije Universiteit Amsterdam, The Netherlands, 1984.
[31] (a) F.M. Bickelhaupt, E.J. Baerends, in: K.B. Lipkowitz, D.B. Boyd (Eds.), Reviews in Computational Chemistry, vol. 15, Wiley–VCH, New York, 2000, p. 1; (b) G. te Velde, F.M. Bickelhaupt, E.J. Baerends, S.J.A. van Gisbergen, C. Fonseca Guerra, J.G. Snijders, T. Ziegler, J. Comput. Chem. 22 (2001) 931.
[32] Selected examples: (a) T. Ziegler, V. Tschinke, A.D. Becke, J. Am. Chem. Soc. 109 (1987) 1351; (b) T. Ziegler, V. Tschinke, C. Ursenbach, (1987). J. Am. Chem. Soc. 109 (1987) 4825; (c) J. Li, G. Schreckenbach, T. Ziegler, J. Am. Chem. Soc. 117 (1995) 486; (d) A.W. Ehlers, E.J. Baerends, F.M. Bickelhaupt, U. Radius, Chem. Eur. J. 4 (1998) 210.
[34] (a) T.K. Firman, C.R. Landis, J. Am. Chem. Soc. 120 (1998) 12650; (b) C.A. Bayse, M.B. Hall, J. Am. Chem. Soc. 121 (1999) 1348.
[35] Ch. Elschenbroich, A. Salzer, Organometallics, 2nd ed., VCH, Weinheim, 1992, p. 227.
[36] L. Mond, C. Langer, F. Quincke, J. Chem. Soc. (1890) 749.
[37] J. Weiß, D. Stetzkamp, B. Nuber, R.A. Fischer, C. Boehme, G. Frenking, Angew. Chem. 109 (1997) 95 (Angew. Chem. Int. Ed. Engl. 36 (1997) 70).
[38] W. Uhl, M. Pohlmann, R. Wartchow, Angew. Chem. 110 (1998) 1007 (Angew. Chem. Int. Ed. Engl. 37 (1998) 961).
[39] H. Braunschweig, C. Kollann, U. Englert, Angew. Chem. 110 (1998) 3355 (Angew. Chem. Int. Ed. Engl. 37 (1998) 3179).
[40] For reviews about Group-13 diyl complexes see: (a) G.J. Irvine, M.J.G. Lesley, T.B. Marder, N.C. Norman, C.R. Rice, E.G. Robins, W.R. Roper, G.R. Whittell, L.J. Wright, Chem. Rev. 98 (1998) 2685; (b) H. Braunschweig, Angew. Chem. 110 (1998) 1882; Angew. Chem. Int. Ed. Engl. 37 (1998) 1786; (c) B. Wrackmeyer, Angew. Chem. 111 (1999) 817; Angew. Chem. Int. Ed. Engl. 38 (1999) 771; (d) R.A. Fischer, J. Weiß, Angew. Chem. 111 (1999) 3002; Angew. Chem. Int. Ed. Engl. 38 (1999) 2830.
[41] G. Frenking, J. Uddin, W. Uhl, M. Benter, S. Melle, W. Saak, Organometallics 18 (1999) 3778.
[42] J. Su, X.-W. Li, R.C. Crittendon, C.F. Campana, G.H. Robinson, Organometallics 16 (1997) 4511.
[43] F.A. Cotton, X. Feng, Organometallics 17 (1998) 128.
[44] (a) C. Boehme, G. Frenking, Chem. Eur. J. 5 (1999) 2184; (b) J. Uddin, C. Boehme, G. Frenking, Organometallics 19 (2000) 571; (c) C. Boehme, J. Uddin, G. Frenking, Coord. Chem. Rev. 197 (2000) 249.
[45] In Ref. [21] we report also about the complexes $(CO)_4Fe–EMe$. The results are very similar to those of the complexes $(CO)_4Fe–EPh$.
[46] (a) T.J. Kealy, P.L. Pauson, Nature 168 (1951) 1039; (b) S.A. Miller, J.A. Tebboth, J.F. Tremaine, J. Chem. Soc. (1952) 632.
[47] (a) G. Wilkinson, J. Am. Chem. Soc. 74 (1952) 2125; (b) R.B. Woodward, J. Am. Chem. Soc. 74 (1952) 3458; (c) E.O. Fischer, Z. Naturforsch. b 7 (1952) 377.
[48] The calculations predict that the reaction $Fe(\eta^5\text{-}N_5)_2 \rightarrow Fe + 5N_2$ is 226.8 kcal mol^{-1} exotherm [22].
[49] A.H. Cowley, V. Lomeli, A. Voigt, J. Am. Chem. Soc. 120 (1998) 6401.
[50] We did not calculate the preparation energies and bond dissociation energies because the multiply charged species do not dissociate into $TM^q + 6CO$.